Journal of Power Sources 195 (2010) 3025–3030

Contents lists available at ScienceDirect

Journal of Power Sources

journal homepage: www.elsevier.com/locate/jpowsour

Short communication

Improvement of the electrochemical properties via poly(3,4-ethylenedioxythiophene) oriented micro/nanorods

Yu Li[a,b], Bichen Wang[a,b], Huimin Chen[a,b], Wei Feng[a,b,*]

[a] School of Materials Science and Engineering, Tianjin University, Tianjin 300072, PR China
[b] Tianjin Key Laboratory of Composite and Functional Materials, Tianjin 300072, PR China

ARTICLE INFO

Article history:
Received 22 June 2009
Received in revised form
16 November 2009
Accepted 18 November 2009
Available online 22 November 2009

Keywords:
Poly(3,4-ethylenedioxythiophene)
Micro/nanorods
Galvanostatic
Cetyltrimethylammonium bromide
Supercapacitor

ABSTRACT

Arrays of oriented poly(3,4-ethylenedioxythiophene) (PEDOT) micro/nanorods are synthesized by electrochemical galvanostatic method at the current density of 1 mA cm^{-2} in the cetyltrimethylammonium bromide (CTAB) aqueous solution whose pH value is 1. The CTAB is used both as the surfactant and the supporting salt in the electrolyte solution. The electrochemical properties of PEDOT films are characterized by cyclic voltammetry and galvanostatic charge/discharge techniques, which indicate that the arrays of oriented PEDOT micro/nanorods can be applied as the electrode materials of supercapacitors. In addition, the cycling performance of PEDOT micro/nanorods is much better than that of traditional PEDOT particles. The effects of the concentration of CTAB, the current density, and pH value of electrolyte solutions on the morphologies and electrochemical properties of PEDOT films are investigated. The mechanism of different morphologies formation is discussed in this study as well.

1. Introduction

The well-known poly(3,4-ethylenedioxythiophene) (PEDOT), as one of the most successful conducting polymers, has been attracting great attention due to its outstanding properties, including high electrical conductivity, high optical transparency in the doped state, good environmental and thermal stability, and electrochemical stability upon cycling [1–4]. These superb properties facilitate it to be applied in the areas of supercapacitors, solar cell, sensors, electrochromic devices, etc. [5–8].

However, the supercapacitors made by conducting polymers need hundreds of seconds or even more time to be charged, which is the main problem to obstacle them to be widely used [9,10]. Nanostructured materials, such as nanotubes, nanowires, random nanoporous structures, and the like, can provide intrinsically broad surface area and shorter diffusion distances for ion transport, which leads to high charge/discharge capacities and fast charge/discharge rates [11]. Martin's group, one of the pioneers in achieving a fast charge/discharge rate of battery materials, has reported that they enhanced charge transport rates of battery by using the one-dimensional (1D) nanomaterials via template synthesis [12]. Liu et al. reported PEDOT nanotubes, which were electrochemically synthesized in a nanoporous alumina, had the fast charge/discharge capability and the potential of being used as a high-powered supercapacitor [13].

There have been many reports about synthesizing 1D conducting polymers by electrochemical polymerization [14,15]. For example, Wei synthesized nanofiber arrays of polypyrrole (PPy) with controlled lengths by a biphasic electrochemical strategy and PPy conical nanocontainer on Pt electrode [15,16]. However, the 1D nanostructured PEDOT was always synthesized by electrochemical polymerization via hard-template [13,17,18] or by oxidative polymerization via soft-template [19,20]. There is rare 1D nanostructured PEDOT electrochemically polymerized via soft-template. In this work, oriented 1D PEDOT micro/nanorods arrays are synthesized by galvanostatic techniques on tantalum electrochemically, while cetyltrimethylammonium bromide (CTAB) is used both as the surfactant and the supporting salt. The influence of the CTAB concentration, the electrolyte pH value and the current density to the morphologies is investigated and the different morphologies formation mechanism is also discussed. The electrochemical properties and the cycling performance of synthesized PEDOT are also characterized and the results indicate that oriented PEDOT micro/nanorods arrays can be used as the ideal materials of supercapacitors.

* Corresponding author at: School of Materials Science and Engineering, Tianjin University, No. 92 Weijin Road, Tianjin 300072, PR China. Tel.: +86 22 87402059; fax: +86 22 27404724.
E-mail address: weifeng@tju.edu.cn (W. Feng).

0378-7753/$ – see front matter © 2009 Elsevier B.V. All rights reserved.
doi:10.1016/j.jpowsour.2009.11.074

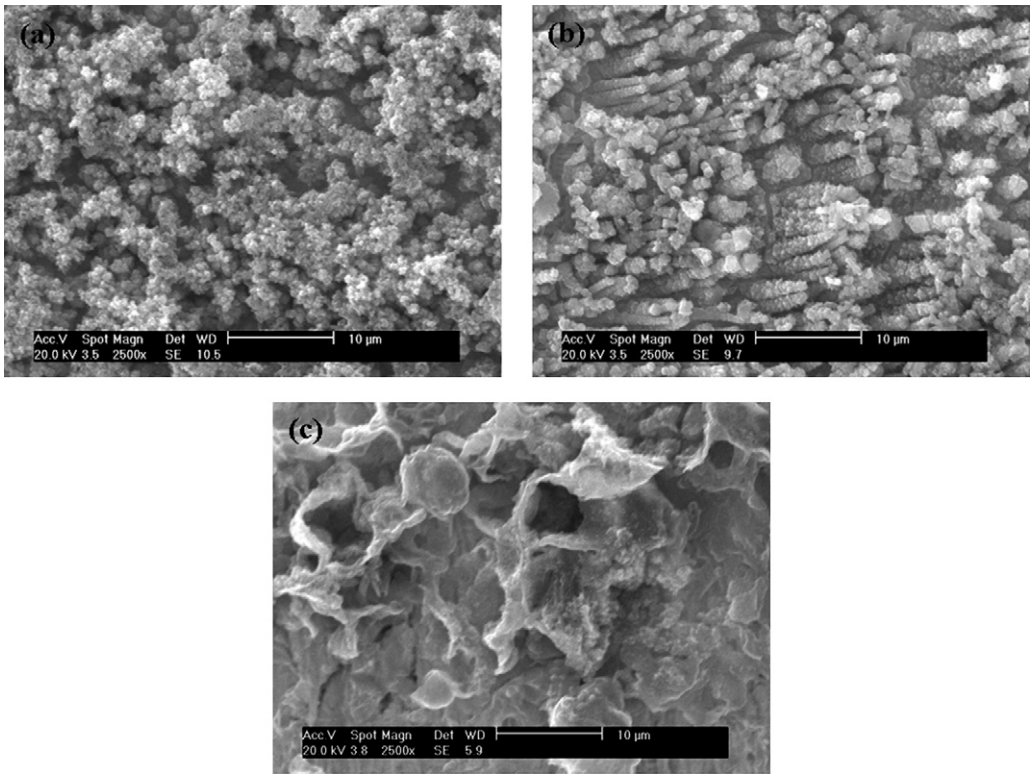

Fig. 1. SEM images of PEDOT electrode prepared by galvanostatic method at the current density of 1.0 mA cm^{-2} in 0.0025 M CTAB (a), 0.01 M CTAB (b), and 0.03 M in pH 1 (c).

2. Experimental details

2.1. Materials

3,4-Ethylenedioxythiophene (EDOT) was purchased from Bayer AG. CTAB was purchased from Tokyo Chemical Industry Co. Ltd. All other reagents were obtained from Tianjin Chemical Company. All reagents were of analytical grade and were used without any further purification.

2.2. Preparation procedures

Tantalum foils (Ta, 10 mm × 10 mm × 0.1 mm), as electrodes which PEDOT deposited on, were rinsed by acetone and deionized water alternately more than three times and dried at 60 °C for 6 h. The aqueous solution containing 0.1 M EDOT and some amount of CTAB was prepared and the pH value was adjusted by HCl. PEDOT films grew on tantalum foil in the prepared solutions by galvanostatic techniques at different current densities and the consumed charge was 2 C. All experiments were conducted at 0–5 °C. After polymerization, electrodes of PEDOT were cleaned by acetone and deionized water alternately more than three times, and then cleaned in 1 M KCl aqueous solution by cyclic voltammetry for one cycle in order to remove the remaining CTAB and EDOT.

2.3. Characterization

The morphologies were characterized by scanning electron microscope (SEM) taken by a PHILIPS XL30ESEM. The electrochemical polymerization and performances of cyclic voltammetry (CV), and galvanostatic charge/discharge techniques were measured with a Potentiostat/Galvanostat (TD73000, Tianjin Zhonghuan Co. Ltd., China) equipped with a conventional three-electrode cell. A PEDOT film was applied as the working electrode, and a platinum foil (Pt, 20 mm × 15 mm × 0.1 mm) served as the counter electrode and an Ag/AgCl (in saturated KCl solution) was used as the reference electrode.

3. Results and discussion

3.1. Morphologies

The morphologies of PEDOT film synthesized by galvanostatic technique were always micro/nanoparticles [21]. However, when CTAB was introduced into the electrolyte, the morphologies of PEDOT film are totally different, whose SEM images are shown in Fig. 1. Arrays of oriented PEDOT micro/nanorods structure, without particles, are synthesized in an aqueous solution containing 0.01 M CTAB, 0.01 M EDOT, and 0.1 M HCl when the current density was 1 mA cm^{-2}. The diameter of micro/nanorods ranges from 0.5 to 0.8 μm and the length ranges from 8 to 10 μm. Nevertheless, the morphology of PEDOT turns to particles when the CTAB concentration is 0.0025 M; whereas, the morphology of PEDOT becomes the tracked blocks when the concentration of CTAB electrolyte increases to 0.03 M.

Arrays of oriented PEDOT micro/nanorods are proposed to be synthesized by the self-assembled micellar soft-template approach. In the beginning, when the concentration of CTAB is low, the cation surfactant CTAB produces an aqueous micellar solution with spherical micelles. The EDOT monomers existing in the electrolyte migrate into the spherical micelles due to their hydrophobic property, where the monomers are electrochemically polymerized to PEDOT particle. With further increasing the CTAB concentration, the spherical micelles turn into an ellipsoidal shape, and then into a rod-like shape, for accommodating more surfactant molecules and minimizing the free energy of the electrolyte solution [22,23]. In this situation, the EDOT monomers are coated by CTAB molecules almost, except the two ends of the rod-like micelles [24], where are the only active points left to process the polymerization. It means that, PEDOT only grows from the ends of rod-like micelles

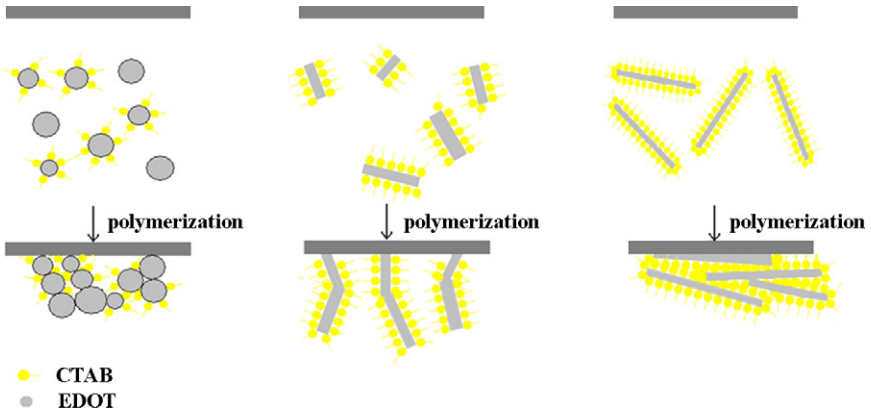

Fig. 2. The mechanism of the formation of PEDOT in particle, rod-like, and block structure.

and PEDOT oriented micro/nanorods arrays form finally. The transition from rod-like to plate-like micelles is the result of more CTAB molecules exiting. That is why the morphology of PEDOT is stacked blocks in the 0.03 M CTAB solution, as shown in Fig. 2c.

The effects of pH value and current density to the morphologies of PEDOT film are also investigated. With the increase of pH value, the PEDOT morphology turns to be stacked blocks (Fig. 3b) and it hardly forms an integrated PEDOT film in the neural electrolyte solution (Fig. 3c). It is because that the dissociation balance of CTAB solution is different when the pH value of electrolyte is changed. As a result, the solubility of CTAB reduces with the increase of pH value and the formation of PEDOT film is restrained. The PEDOT micro/nanorods can also form when the current density of electrochemical polymerization is 1 and 2 mA cm^{-2} (Fig. 4b and c). But only PEDOT random structures exist at a lower current density (Fig. 4a) and PEDOT stacked blocks exist at a higher current density (Fig. 4d). The slower rate of the nucleation and the growth lead to the orderly growth of PEDOT and the formation of oriented micro/nanorods arrays. However, when the current density is 0.5 mA cm^{-2}, the rate of the nucleation and the growth of PEDOT are so slow that EDOT monomers only can be initiated to polymerize from the limited active nucleus, leading to the random structure. When the current density is 5 mA cm^{-2}, the rate of nucleation and the growth of PEDOT both accelerate. Therefore, more nucleation sites exist on the work electrode and PEDOT grow in all directions, thus resulting in randomly stacked blocks rather than the oriented micro/nanorods.

3.2. Cyclic voltammetrical analysis

The CV curves of PEDOT film with the structure of micro/nanorods, particles, and stacked blocks, which were obtained in 0.01, 0.005, and 0.03 M CTAB solution, respectively, are shown in Fig. 5. All cyclic voltammetric ranges are performed

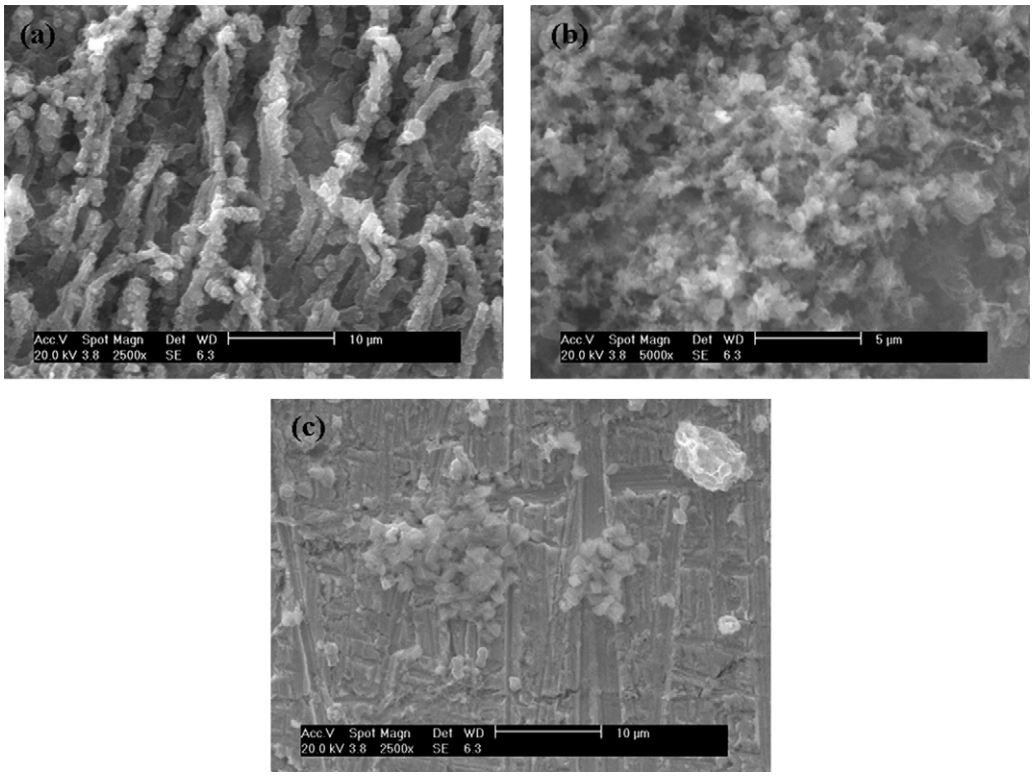

Fig. 3. SEM images of PEDOT electrode prepared by galvanostatic method at the current density of 1.0 mA cm^{-2} in 0.01 M CTAB with pH 1 (a), pH 3 (b), and pH 5 (c).

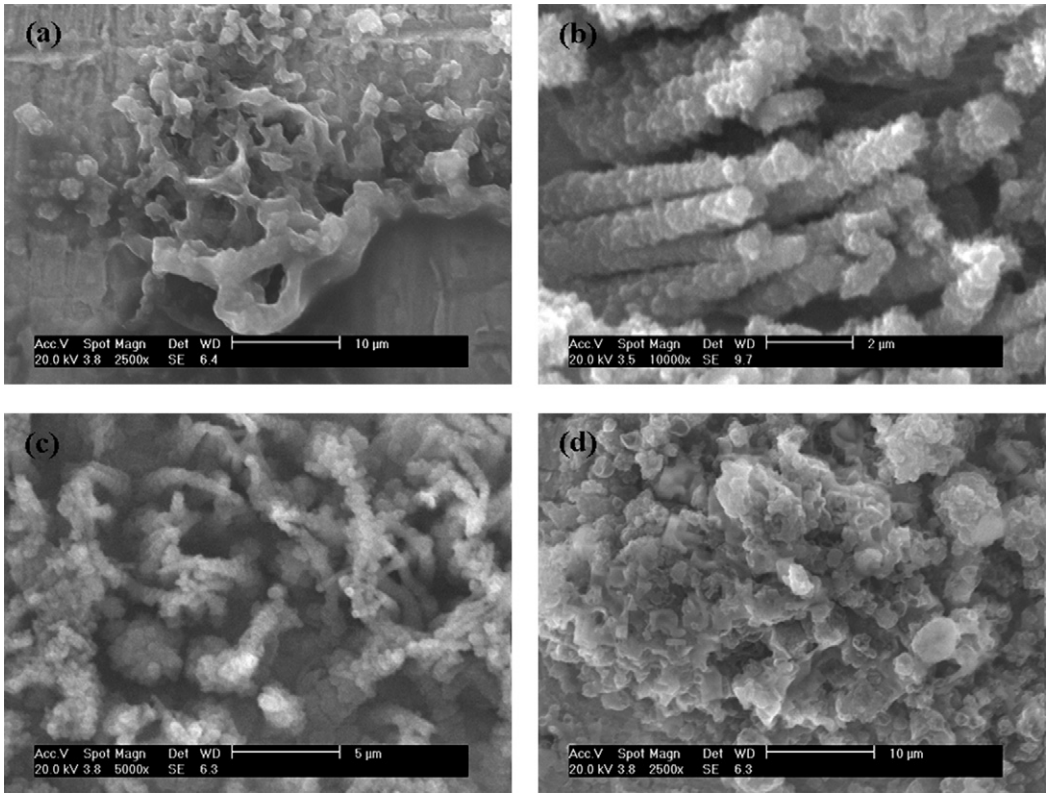

Fig. 4. SEM images of PEDOT electrode prepared by galvanostatic method in the solution of pH 1 and 0.01 M CTAB at 0.5 mA cm^{-2} (a), 1.0 mA cm^{-2} (b), 2.0 mA cm^{-2} (c), and 5.0 mA cm^{-2} (d).

from −0.4 to 0.6 V in 1 M KCl aqueous solution, with the scan rate of 50 mV s^{-1} in three-electrode system. It is obvious that the CV shapes of PEDOT micro/nanorods and particles are similar to the ideal supercapacitor's behavior, while that of PEDOT blocks are not so good. The curve of PEDOT micro/nanorods displays a rectangle-like shape, which means a fast electrochemical switch.

The specific capacitance (C_m) values of these PEDOT films were calculated from the CV curves by using the following Eq. (1):

$$C_m = \frac{i}{v \times m} \quad (1)$$

where i is the average current, v is the scan rate and m is the mass of PEDOT film [25]. The specific capacitance of PEDOT micro/nanorods, particles, and tracked blocks is 86.80, 29.44 and 15.22 F g^{-1}, respectively. The specific capacitance of PEDOT micro/nanorods is much higher than that of PEDOT particles and blocks, which indicates that the microstructure influences significantly to electrochemical properties of PEDOT [19,26]. It is known that the micro/nanorods will facilitate the contact between the electrolyte and the active sites of the film. In addition, 1D morphology not only can provide broader surface area than that of the traditional granular morphology but also shorten the shorter diffusion distances for ion transport, which leads to high charge/discharge capacities as well as fast charge/discharge rates [11]. So the average specific capacitance of PEDOT micro/nanorods morphology is significantly higher than that of PEDOT particles or blocks. The similar conclusion was reported that the hybrid films of polyaniline and manganese oxide in nanofibrous morphology have a higher specific capacitance [27].

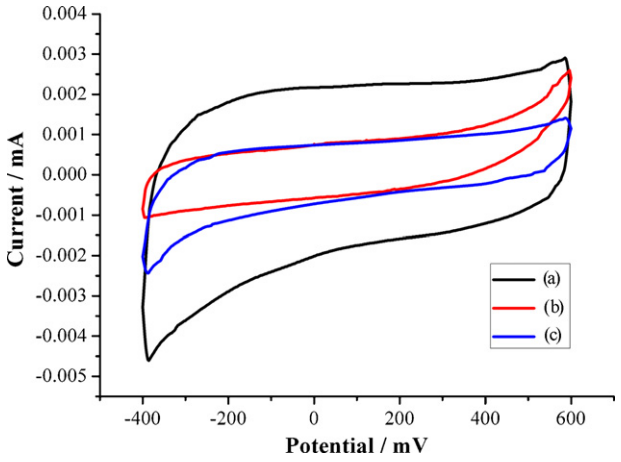

Fig. 5. CV curves of PEDOT micro/nanorods (a), particles (b), stacked blocks, and (c) in 1 M KCl solution at scan rate of 50 mV s^{-1} in 1 M KCl with three-electrode system.

Charge/discharge rate can be further evaluated by performing the CV scans at different scanning rates. Fig. 6 shows the specific capacitance of PEDOT electrodes with arrays of oriented micro/nanorods structure at different scan rates ranging from 10 to 200 mV s^{-1} in 1 M KCl solution. The curve shapes at 10, 50 mV s^{-1}, and even 200 mV s^{-1} are all close to rectangle, although the specific capacitance decreases slightly with the increase of scanning rate.

3.3. Galvanostatic charge/discharge

The process of charge/discharge and the specific capacitance of different structures of PEDOT are studied as well. Fig. 7 presents the charge/discharge curves of the PEDOT micro/nanorods, particles, and stacked blocks at a constant current 1 A g^{-1} between 0 and 0.6 V in 1 M KCl in three-electrode system. The potential of the PEDOT micro/nanorods varies almost linearly with time during the whole charging and discharging processes, and there is a visible voltage drop at the beginning of the discharge process, which is

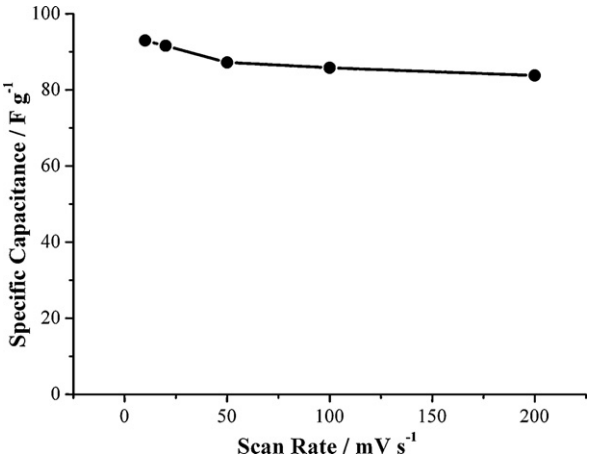

Fig. 6. Plots of PEDOT micro/nanorods specific capacitance versus scan rate.

a characteristic behavior of ideal supercapacitor. Comparing with the other two, it also performs both longer charge and discharge time, which confirms it has a better capacitance behavior. The C_m is calculated from the galvanostatic charge/discharge curves by the following Eq. (2):

$$C_m = \frac{i \times \Delta t}{m \times \Delta V} \quad (2)$$

where i is the constant current, Δt is the time interval for the change in voltage ΔV, and m is the mass of PEDOT film. The discharge specific capacitances of PEDOT micro/nanorods, particles, and stacked blocks are calculated to be 109.11, 72.52 and 36.77 F g^{-1}, respectively, which are similar to the results obtained from CV curves at 10 mV s^{-1}. This high linearity and symmetry in the galvanostatic charge/discharge curve of PEDOT micro/nanorods film in Fig. 7a indicates the high charge/discharge efficiency (η) of 90.7%, which is the ratio of discharge time t_d and charge time t_c [13]. This enhanced response rate may be attributed to the special oriented micro/nanorods structure, which provide boarder room and shorter diffusion distances for ion transport between electrolyte and PEDOT film.

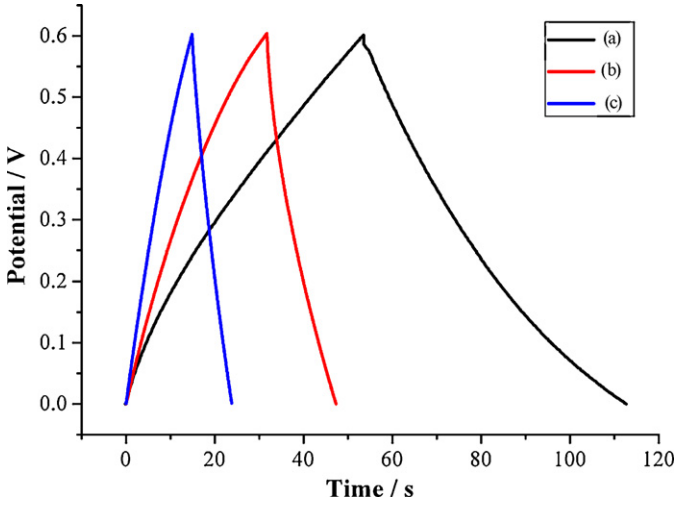

Fig. 7. Galvanostatic charge/discharge curves of PEDOT micro/nanorods (a), particles (b), stacked blocks, and (c) at 1 A g^{-1} in 1 M KCl with three-electrode system.

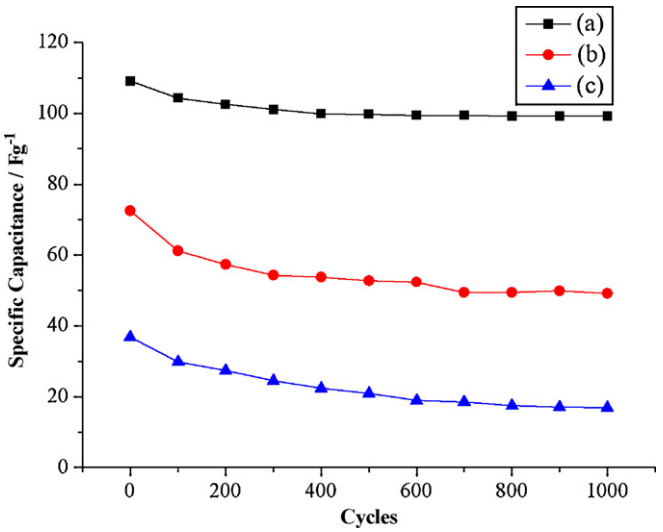

Fig. 8. Cycling test of PEDOT micro/nanorods (a), particles (b), stacked blocks, and (c) at 1 A g^{-1} in 1 M KCl with three-electrode system.

3.4. Cycling performance

As it is well-known, the long-term stability of conducting polymers is an important consideration for their applications in supercapacitors. The cycling performance of different structures of PEDOT is tested by the charge/discharge technique in 1 M KCl solution at a constant current density of 1 A g^{-1} in the three-electrode system. Fig. 8 presents the cycling performance of the PEDOT micro/nanorods, particles, and stacked blocks. It can be observed that PEDOT micro/nanorods have no drift of specific capacitance in the whole cycling test and the specific capacitance decays slowly from 109.11 to 99.15 F g^{-1}. This means that the capacity fades at 1000th cycle for PEDOT micro/nanorods are just 9.13%. However, under the same test condition, the capacity of PEDOT particles and stacked blocks fades at 1000th cycle is 32.27% and 54.09%, respectively, comparing with their original values. Comparing with these results, PEDOT micro/nanorods have much better cycling performance. The remarkable improved cycling performance of PEDOT micro/nanorods can be attributed the special 1D structure, which offers a higher specific surface area that is convenient for ions accessing into the polymer matrix and inducing higher charge to keep stable, as well as provides broad interspaces among each micro/nanorods that avoids PEDOT film to be destroyed by volume swelling or shrinking during the cycling charge/discharge process [28]. Moreover, a simultaneous p-doping reaction may occur during the polymeric process, which is more stable than n-doping polymer [29].

4. Conclusion

PEDOT film with arrays of oriented micro/nanorods has been synthesized by galvanostatic techniques at 1 mA cm^{-2} current density in aqueous solution containing 0.1 M EDOT, 0.01 M CTAB, and HCl (which is used to adjust pH value of electrolyte to 1). This study provides a convenient method to prepare PEDOT with special morphologies through an environment friendly way. The influences of the CTAB concentration, the electrolyte pH value and the current density to the morphologies are investigated and the different morphologies formation mechanism are also discussed. PEDOT electrode with micro/nanorods structure shows an excellent specific capacitance and a stable cycling performance, which demonstrates that arrays of oriented micro/nanorods PEDOT are a kind of very promising electrode material for supercapacitors.

Acknowledgments

This work was partly supported by the National Basic Research Program of China (2010CB934700), the National Natural Science Foundation of China (No. 50873074), the Program for New Century Excellent Talents in University of Chinese Education Ministry (No. 060232) and the Key Project of Chinese Ministry of Education (No. 108029).

References

[1] W.J. Bjorn, W. Keld, Macromolecules 37 (2004) 4538–4543.
[2] C. Pinar, T. Simge, S. Ertugrul, M.A. Idris, T. Cihangir, T. Levent, Sol. Energy Mater. Sol. Cells 92 (2008) 154–159.
[3] I. Winter, C. Reese, J. Hormes, G. Heywang, F. Jonas, Chem. Phys. 194 (1995) 207–213.
[4] F. Wang, S.M. Wilson, R.D. Rauh, Macromolecules 33 (2000) 2083–2091.
[5] S. Patra, N. Munichandraiah, J. Appl. Polym. Sci. 106 (2007) 1160–1171.
[6] Y.J. Yang, Y.D. Jiang, J.H. Xu, J.S. Yu, Polymer 48 (2007) 4459–4465.
[7] A.A. Argun, A. Cirpan, J.R. Reynold, Adv. Mater. 15 (2003) 1338–1341.
[8] A. Burke, J. Power Sources 91 (2000) 37–50.
[9] P.J.S. Foot, F. Mohammed, P.D. Calvert, N.C. Bilingham, J. Phys. D: Appl. Phys. 20 (1987) 1354–1360.
[10] R.M. Penner, L.S. Van Dyke, C.R. Martin, J. Phys. Chem. 92 (1988), 5274-5182.
[11] S.I. Cho, S.B. Lee, Accounts Chem. Res. 41 (6) (2008) 699–707.
[12] Z.H. Cai, C.R. Martin, Synth. Met. 46 (1992) 165–179.
[13] R. Liu, I.C. Seung, B.L. Sang, Nanotechnology 19 (2008) 215710.
[14] L. Liang, J. Liu, F. Charles, J. Windisch, J.E. Gregory, Y.H. Lin, Chem. Int. Ed. 41 (2002) 3665–3668.
[15] M. Li, Z.X. Wei, L. Jiang, J. Mater. Chem. 18 (2008) 2276–2280.
[16] J.Y. Huang, B.G. Quan, M.J. Liu, Z.X. Wei, L. Jiang, Macromol. Rapid Commun. 29 (2008) 1335–1340.
[17] J.L. Duvaila, P. Retho, S. Garreaua, G. Louarna, C. Godona, C.S. Demoustier, Synth. Met. 131 (2002) 123–128.
[18] M.R. Abidian, D.H. Kim, D.C. Martin, Adv. Mater. 18 (2006) 405–409.
[19] W. Feng, Y. Li, J. Wu, N. Hideki, A. Fujii, M. Ozaki, K. Yoshino, J. Phys.: Condens. Matter 19 (2007) 186220.
[20] S. Nair, E. Hsiao, S.H. Kim, Chem. Mater. 21 (2009) 115–121.
[21] J. Wang, Y.L. Xu, X.F. Sun, X.F. Li, J. Solid State Electrochem. 12 (2008) 947–952.
[22] P.A. Hassan, K. Bhattacharya, S.K. Kulshreshtha, S.R. Raghavan, J. Phys. Chem. B 109 (2005) 8744–8748.
[23] S. Trabelsi, P.A. Albouy, I.C. Marianne, S. Guillot, D. Langevin, Chem. Phys. Chem. 8 (2007) 2379–2385.
[24] H. Habazaki, M. Kiriu, M. Hayashi, H. Konno, Mater. Chem. Phys. 101 (2007) 367–372.
[25] D.K. Bhat, M.S. Kumar, J. Mater. Sci. 42 (2007) 8158–8162.
[26] J.W. Long, B. Dunn, D.R. Rolison, H.S. White, Chem. Rev. 104 (2004) 4463–4492.
[27] L.J. Sun, X.X. Liu, K.T. Kim, L. Chen, W.M. Gu, Electrochim. Acta 53 (2008) 3036–3042.
[28] L. Li, D.C. Loveday, D.S.K. Mudigonda, J.P. Ferraris, Electrochem. Soc. 149 (2002) A472–477.
[29] J.P. Zheng, T.R. Jow, J. Power Sources 62 (1996) 155–159.